PHYSICAL REVIEW C **76**, 052802(R) (2007)

New ^{30}P$(p,\gamma)^{31}$S resonances and oxygen-neon nova nucleosynthesis

C. Wrede,[1,*] J. A. Caggiano,[2,†] J. A. Clark,[1] C. Deibel,[1] A. Parikh,[1,‡] and P. D. Parker[1]
[1]*Wright Nuclear Structure Laboratory, Yale University, New Haven, Connecticut 06520, USA*
[2]*TRIUMF, Vancouver, British Columbia V6T 2A3, Canada*
(Received 12 August 2007; published 19 November 2007)

Enriched isotopic abundance ratios of ^{30}Si/^{28}Si in several presolar SiC and graphite grains qualitatively indicate massive oxygen-neon (ONe) nova origins but fall short of hydrodynamic ONe nova model ejecta predictions by as much as an order of magnitude. The astrophysical ^{30}P$(p,\gamma)^{31}$S reaction rate uncertainty at ONe nova temperatures ($0.10 < T < 0.35$ GK) spans several orders of magnitude through which the predicted amount of ejected ^{30}Si can vary by a factor of 100. By measuring triton momenta from the ^{31}P(^{3}He,t)^{31}S reaction at 20 MeV, the energies of ^{30}P $+p$ resonances in the Gamow window for ONe novae have been determined to better than ± 3 keV, and two new resonances at $E_{\mathrm{c.m.}} = 194.0(25)$ and 266.4(27) keV that likely dominate the ^{30}P$(p,\gamma)^{31}$S rate for $0.08 < T < 0.25$ GK have been resolved. A resulting increase in the experimentally determined ^{30}P$(p,\gamma)^{31}$S reaction rate puts it in accord with Hauser-Feshbach statistical model estimates for $0.08 < T < 0.40$ GK, supporting conclusions drawn from ONe nova model studies that employed a Hauser-Feshbach rate.

DOI: 10.1103/PhysRevC.76.052802 PACS number(s): 26.30.+k, 97.30.Qt, 25.55.Kr, 27.30.+t

The uncertain ^{30}P$(p,\gamma)^{31}$S reaction rate in oxygen-neon (ONe) novae influences predicted ejecta abundances [1,2] in the Si-Ca mass region, which are observed [3–5] using optical astronomy and measured [6,7] in presolar grains [8]. Several presolar SiC and graphite grains believed to be of nova origin [6,7] have ^{30}Si/^{28}Si ratios in excess of the solar abundance by factors of 1.04–2.11. The predicted value of this ratio [1] is sensitive to the rate of the ^{30}P$(p,\gamma)^{31}$S reaction because ^{30}P can either capture a proton to form ^{31}S (initiating a path of nucleosynthesis that is unlikely to form ^{30}Si) or β decay ($t_{1/2} = 2.5$ min) to ^{30}Si.

Until 2006, the only available rates for the ^{30}P$(p,\gamma)^{31}$S reaction in ONe novae were based on Hauser-Feshbach (HF) statistical model calculations (e.g., [9–12]). Using a HF rate [11], hydrodynamic models of ONe novae [7] on massive (1.25–1.35$M_\odot$) white dwarfs yield ^{30}Si/^{28}Si ejecta ratios 2.4–9.2 times the solar value, qualitatively consistent with presolar grain measurements. The predicted ^{30}Si/^{28}Si ejecta ratio can be tuned to agree quantitatively with measurements by invoking mixing with solar composition material [7] or by increasing the ^{30}P$(p,\gamma)^{31}$S reaction rate. The rate may deviate significantly from HF estimates that may not be reliable for a nucleus as light as ^{31}S at the relatively low temperatures of ONe novae where a few resonances could dominate [2]. Therefore, an experimental determination is required to constrain nucleosynthesis in ONe nova models.

In a stellar environment where particles have a Maxwell-Boltzmann distribution of energies characterized by temperature T, the resonant ^{30}P$(p,\gamma)^{31}$S reaction rate per particle pair [13] is given by a sum over narrow, isolated resonances r,

$$\langle \sigma \upsilon \rangle = \left(\frac{2\pi}{\mu k T}\right)^{3/2} \hbar^2 \sum_r (\omega\gamma)_r e^{-E_r/kT}, \qquad (1)$$

where $\hbar$ is the Dirac constant, k is the Boltzmann constant, μ is the reduced mass, and E_r are the resonance energies in the c.m. frame.

$$(\omega\gamma)_r = \frac{(2J_r+1)}{(2J_p+1)(2J_P+1)}\left(\frac{\Gamma_p\Gamma_\gamma}{\Gamma}\right)_r \qquad (2)$$

are the resonance strengths, where $J_p(=1/2)$, $J_P(=1)$ and J_r are the spins of the reactants and the resonance, respectively. Γ_p and Γ_γ are the proton and γ-ray partial widths of the resonance, respectively, and $\Gamma = \Gamma_p + \Gamma_\gamma$ is the total width. Each term in the sum has explicit and implicit (through Γ_p) dependencies on E_r because of the Coulomb barrier.

In 2006, the ^{30}P$(p,\gamma)^{31}$S rate was reevaluated [14] based on available experimental information on ^{31}S, its mirror ^{31}P, and a Gammasphere measurement of high-spin states of these nuclei excited by the ^{12}C(^{20}Ne,n) and ^{12}C(^{20}Ne,p) fusion-evaporation reactions. This was a necessary first step toward determining an experimental ^{30}P$(p,\gamma)^{31}$S reaction rate because a radioactive ^{30}P beam of sufficient intensity is not yet available for proposed direct measurements of resonance strengths (e.g., TRIUMF experiment S1108). A subsequent rate evaluation [15] based on a recent study of the ^{32}S$(p,d)^{31}$S reaction yielded similar results. Two simple improvements can be made on the assessments [14,15] by further measurements using stable beams. First, it is probable that the relevant levels in ^{31}S have not all been discovered because there remain ^{31}P levels without ^{31}S mirror partners in the Gamow window. Consequently, these experimental reaction rates were significantly lower than the HF estimates, compounding the ^{30}Si/^{28}Si discrepancy between models and measurements. Second, four known contributing resonances at $E_r = 124(5)$, 217(11), 410(11), and 460(15) keV are not sufficiently well located in energy, which alone introduces

*christopher.wrede@yale.edu
†Present address: Pacific Northwest National Laboratory, Richland, WA 99352, USA.
‡Present address: Departament de Física i Enginyeria Nuclear, Universitat Politécnica de Catalunya, E-08036 Barcelona, Spain.

an order of magnitude uncertainty in the reaction rate at temperatures below $T = 0.2$ GK and a significant uncertainty above. The experimental evaluations can be advanced by a high-resolution spectroscopic study of ^{30}P + p resonances above the proton threshold of $E_x(^{31}\mathrm{S}) = 6133.0(15)$ keV [16] using transfer or charge-exchange reactions.

We have measured the energies of known resonances and searched for new resonances using the nonselective ^{31}P(^{3}He,t)^{31}S reaction at Yale University's Wright Nuclear Structure Laboratory.

Phosphorus targets were made at Duke University by evaporating ≈160 μg/cm^2 of ^{31}P onto 20 μg/cm^2 carbon substrata mounted on aluminum frames using the two-step vacuum-evaporation method described in Refs. [17,18]. A 125 μg/cm^2 Al foil target was used for calibration of the focal plane during each run. Target thicknesses were determined to an uncertainty of ±10% by measuring the energy loss of 5.486-MeV ^{241}Am-decay α particles through the targets with a silicon surface barrier detector before and after beam exposure.

A tandem Van de Graaff accelerated ^{3}He ions to 20 MeV with intensity up to 50 pnA. An Enge magnetic spectrograph accepted light reaction products through a rectangular aperture of variable solid angle, and momentum analyzed them. Tritons were focused on a detection plane spanned by a position-sensitive ionization drift chamber [19] over radii $70 < \rho < 87$ cm. It measured the position and the energy loss, ΔE, of the particles. The residual energy, E, of particles was deposited into a backing scintillator.

The ^{31}P(^{3}He,t)^{31}S and ^{27}Al(^{3}He,t)^{27}Si reactions were measured over a 5-day period with $B = 9$ kG; spectrograph angles $\theta_{\mathrm{lab}} = 1^\circ, 10^\circ$, and 20°; and horizontal and vertical aperture settings of $\Delta\theta = \pm 10$ mrad and $\Delta\phi = \pm 40$ mrad, respectively. Two additional high statistics measurements (5 days each) at 8.5 kG were made with (θ_{lab}, $\Delta\theta$, $\Delta\phi$) = (1°, ±10 mrad, ±40 mrad) and (1.5°, ±20 mrad, ±40 mrad). These additional runs were part of a ^{31}P(^{3}He,t)^{31}S*(p)^{30}P measurement that will be published separately [20].

Particle groups (p, d, t, α) were identified by combining ρ, ΔE, and E in two-dimensional histograms. Tritons were selected cleanly by sorting the data offline through software gates in these histograms, and spectra of focal-plane position were plotted for the ^{31}P(^{3}He,t)^{31}S (Fig. 1) and ^{27}Al(^{3}He,t)^{27}Si reactions.

Kinematic analysis of the triton spectra yielded no evidence of background peaks from (^{3}He,t) reactions on target contaminants. At $B = 8.5$ and 9 kG, tritons from the ^{12}C(^{3}He,t) and ^{16}O(^{3}He,t) reactions were excluded at the detector position. The ^{13}C(^{3}He,t) reaction produced a diffuse, low-intensity background that was determined to be negligible from measurements with an enriched ^{13}C target. Use of a melamine ($C_3H_6N_6$) target showed that nitrogen presented no significant background.

The spectra were analyzed using a least-squares fit of multiple ≈25 keV-FWHM Gaussian and exponentially modified Gaussian (asymmetric to account for a low-energy triton tail) functions, from which peak centroids were determined. The two independent fits produced consistent excitation energies. There was no evidence for resonances with widths comparable to the instrumental resolution or greater, so peak widths were held fixed to a value determined by fitting isolated peaks.

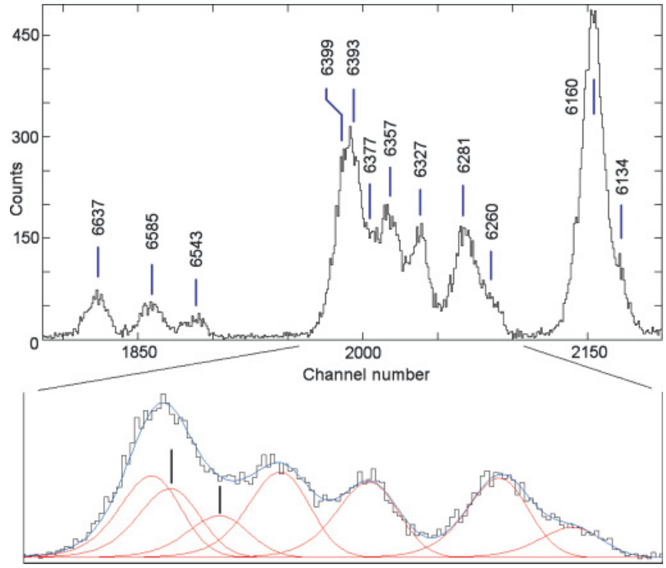

FIG. 1. (Color online) Focal-plane triton spectrum from the ^{31}P(^{3}He,t)^{31}S reaction, corresponding to adopted $E_x(^{31}\mathrm{S}) \approx$ 6100–6700 keV (labeled). The spectrum was acquired with $\theta_{\mathrm{lab}} = 1.5^\circ$, $\Delta\theta = \pm 20$ mrad, and $\Delta\phi = \pm 40$ mrad. Magnified: the overall best fit (blue online) and seven constituent exponentially modified Gaussian peaks (red online). The positions of the 6376.9 and 6393.3 keV peaks (markers) and the widths of all peaks were held fixed. For the spectrum shown, the relative population of the 6393 keV peak to the 6399 keV peak was determined to be 0.84 ± 0.40.

Isolated, easily identifiable excited states of ^{27}Si in the range $5 < E_x < 9$ MeV [from the ^{27}Al(^{3}He,t)^{27}Si reaction] with uncertainties as low as ±0.4 keV (but typically ±3 keV) were used for an initial calibration of the focal plane at each angle. Second-order polynomial least-squares fits of ρ to focal plane position (with $\chi^2_\nu = 0.94$-1.32) were derived from known ^{27}Si excitation energies [21] and measured peak centroids. These fits were used to identify and determine ^{31}S excitation energies to an uncertainty of ±3 keV. Precisely known ^{31}S levels[1] at 5978.2(7) keV, 6160.2(7) keV, 6636.3(15) keV, and 7302.8(8) keV [14] were then used for an internal calibration of the ^{31}S spectra with $\chi^2_\nu = 0.56$–1.99 (fits for the two high statistics spectra, which carry the most weight, had $\chi^2_\nu = 0.56$ and 0.73). This eliminated systematic uncertainties associated with using a different target for the calibration and yielded a ±2 keV excitation energy uncertainty. The results were consistent with those from the ^{27}Si calibration and are summarized in Table I.

All known ^{31}S states from the proton threshold to 6.7 MeV were populated, three previously unresolved resonances were excited, and the existence of a 6585(2) keV level observed to date only tentatively was confirmed [25].

[1]Where excitation energy uncertainties are not quoted directly in Ref. [14], they are derived from the constituent γ-ray energy uncertainties in Ref. [14].

TABLE I. ^{31}S energy levels. Adopted energies (keV) are derived from a weighted average of this work with past work. J^π assignments are a combination of past work and possible mirror assignments including the present work.

Endt [21]	(^{3}He,α) [22]	($\beta^+\gamma$) [23]	(^{20}Ne,$n\gamma$) [14]	(p,d) [15]	(^{3}He,t) Present work	E_x Adopted	$J^\pi;T$ Adopted
					6134(2)	6134.0(20)	$(3/2^+ - 9/2^+)$
6155(10)			6160.2(7)[a]		6160(3)[b]	6160.2(7)	$5/2^-$
6267(10)	6257(5)			6267(5)	6259(2)	6259.9(17)	$1/2^+; 1/2$
6268(10)		6280(2)			6283(2)	6281.2(14)	$3/2^+; 3/2$
					6327(2)	6327.0(20)	$(3/2^-, 7/2^+)$
6350(11)					6357(2)	6356.8(20)	$(5/2^+)$
			6376.9(5)		[c]	6376.9(5)	$9/2^-$
			6393.7(5)		[c]	6393.3(5)[d]	$11/2^+$
6396(10)	6393(5)			6411(9)	6400(3)[e]	6399.4(22)	$(3/2^-, 5/2^-, 7/2^+)$
6543(11)				6546(15)	6543(2)	6543.1(20)	$(3/2, 5/2)^-$
(6593(15))					6585(2)	6585.1(20)	$(3/2, 5/2, 7/2)^-$
6628(13)			6636.3(15)[a]		6639(3)[b]	6636.8(13)	$9/2^-$

[a]Used in energy calibration.
[b]Determined using ^{27}Si calibration independently of Ref. [14]. The internal calibration yielded 6159(2) and 6637(2) keV.
[c]Populated but held fixed for purposes of fitting, using results of Refs. [14,24].
[d]Weighted average of 6393.7(5) keV and 6391.1(12) keV from Refs. [14] and [24], respectively.
[e]Weighted average of 6401(3) and 6398(6) keV from (^{3}He,t) and (d,t) [20] measurements, respectively.

New levels were observed at 6134(2) keV and 6327(2) keV. These were likely obscured by the 6160 keV and 6357 keV levels, respectively, in previous transfer studies. For example, a high resolution ^{32}S(^{3}He,α)^{31}S spectrum [26] has an unidentified peak at a position corresponding to $E_x \approx$ 6325 keV.

A 6401(3) keV level was found by fitting our two high statistics spectra (Fig. 1) with peaks at the channels corresponding to the known [14,24] levels at 6393.3(5) keV and 6376.9(5) keV fixed in position (Table I). This state was required at the 4.2σ and 3.5σ levels in the spectra at $\theta_{\rm lab} = 1^\circ$ and 1.5°, respectively. Because of the large angular momentum transfer needed, we do not expect the $J^\pi = 11/2^+$, 6393.3(5) keV level to be strongly excited by the ^{32}S(^{3}He,α) [21,22], ^{32}S(p,d) [15], and ^{32}S(d,t) [20] single-nucleon transfer reactions. Therefore we identify the 6401(3) keV level with the levels observed using these reactions (Table I).

To constrain the J^π values of the new ^{31}S levels, we appeal to its mirror ^{31}P. Adopting the ^{31}S–^{31}P mirror partners from previous work [14,21,22] for the 6160, 6260, 6281, 6357, 6377, 6393, and 6637 keV ^{31}S levels, we note that the following ^{31}P levels have not been assigned a ^{31}S partner: [E_x(^{31}P); J^π] = [6233 keV; $(3/2^+ - 9/2^+)$], [6496 keV; $3/2^-$], [6594 keV; $5/2^-$], [6610 keV; $3/2^-$], and [6842 keV; $(5/2, 7/2)^-$]. We also include a 6507(2) keV ^{31}P level [27,28] of unknown spin that was discarded [29] by identifying it with the 6500.6(9) keV ^{31}P level [21] although the two levels have distinct γ-decay branches and their energies are inconsistent. The 6507 keV level is fed by γ decay of the $J = 7/2$, 9865 keV level and has a strong γ-decay branch to the $J^\pi = 5/2^+$, 3295 keV level. Noting also that the recent $J^\pi = 5/2^-$ measurement [14] for the 6399 keV ^{31}P level overturned its $7/2^+_6$ shell-model assignment [21] (displacing the $7/2^+_6$ level), we conjecture $J^\pi = 7/2^+$ for the 6507 keV level. A remeasurement of the γ cascade from the 9865 keV level using the ^{30}Si$(p,\gamma)^{31}$P reaction could confirm or refute the existence of the 6507 keV level. Assuming a typical mirror energy difference MED = $E_x(^{31}\mathrm{S}) - E_x(^{31}\mathrm{P})$ between -250 and 0 keV, we match the new 6134 keV level with the 6233 keV ^{31}P level. The new 6327 keV level could be paired with the 6496 or 6507 keV ^{31}P levels. The new 6399 keV level could be paired with any of the 6496, 6507, 6594, or 6610 keV ^{31}P levels. The 6543 and 6585 keV levels could be paired with the 6594 or 6610 keV ^{31}P levels. If the 6507 keV ^{31}P level does not exist then the 6585 keV level could be paired with the 6842 keV ^{31}P level, which results in a large, but conceivable, MED of -257 keV. For lack of spectroscopic information, we simply match the available levels in order of increasing energy as shown in Fig. 2.

Adopting the ^{31}S excitation energies from Table I, the Q value of 6133.0(15) keV, and the spins indicated by the mirror assignments in Fig. 2, the ^{30}P$(p,\gamma)^{31}$S reaction rate was calculated using Eq. (1). Proton widths were estimated using the formula [13]

$$\Gamma_p = \frac{2\hbar}{R_n}\left(\frac{2E_r}{\mu}\right)^{1/2} P_\ell(E_r, R_n) C^2 S \theta^2_{\rm s.p.}, \qquad (3)$$

where $R_n = 1.25(1^{1/3} + 30^{1/3})$ fm is the interaction radius, $P_\ell(E_r, R_n)$ is the penetration factor that was determined by computing the regular and irregular Coulomb wave functions [13,30], C is an isospin Clebsch-Gordan coefficient, S is the spectroscopic factor, and $\theta^2_{\rm s.p.}$ is the single particle reduced width that was determined using Ref. [31]. C^2S and Γ_γ were adopted from Ref. [14], except we assumed $C^2S = 0.10$ for even-parity resonances where no other information was available. Resonance parameters are summarized in Table II.

The ^{30}P$(p,\gamma)^{31}$S reaction rate (Fig. 3) has increased in comparison with the former evaluations [14,15] by over a factor of 2 for $0.09 < T < 0.32$ GK and by over a factor of 8 for

TABLE II. ^{30}P$(p,\gamma)^{31}$S resonance parameters. See text for details.

E_x (keV)	E_r (keV)	ℓ	$\theta^2_{\text{s.p.}}$	C^2S	Γ_p (keV)	Γ_γ (keV)	$\omega\gamma$ (keV)
6160.2(7)	27.2(17)	1	0.70	0.02	5.19×10^{-34}	$1.5(5) \times 10^{-5}$	5.19×10^{-34}
6259.9(17)	126.9(23)	0	0.55	0.003	9.47×10^{-14}	1.5×10^{-4}	3.16×10^{-14}
		2	0.36	0.015	3.79×10^{-15}	1.5×10^{-4}	1.26×10^{-15}
6281.2(14)	148.2(21)	0	0.55	0.00025	2.08×10^{-13}	1.5×10^{-4}	1.39×10^{-13}
6327.0(20)	194.0(25)	1	0.70	0.02	5.41×10^{-10}	1.5×10^{-4}	3.61×10^{-10}
6356.8(20)	223.8(25)	2	0.36	0.044	3.79×10^{-10}	1.5×10^{-4}	3.79×10^{-10}
6376.9(5)	243.9(16)	3	0.35	0.02	1.34×10^{-11}	$1.2(4) \times 10^{-5}$	2.23×10^{-11}
6393.3(5)	260.3(16)	4	1.00	0.10	5.62×10^{-12}	$2.0(8) \times 10^{-5}$	1.12×10^{-11}
6399.4(22)	266.4(27)	2	0.36	0.10	1.08×10^{-8}	1.5×10^{-4}	1.44×10^{-8}
6543.1(20)	410.1(25)	1	0.70	0.02	1.66×10^{-5}	1.5×10^{-4}	1.50×10^{-5}
6585.1(20)	452.1(25)	1	0.70	0.02	4.78×10^{-5}	1.5×10^{-4}	2.42×10^{-5}
6636.8(13)	503.8(20)	3	0.35	0.02	1.70×10^{-7}	$3.3(7) \times 10^{-6}$	2.69×10^{-7}

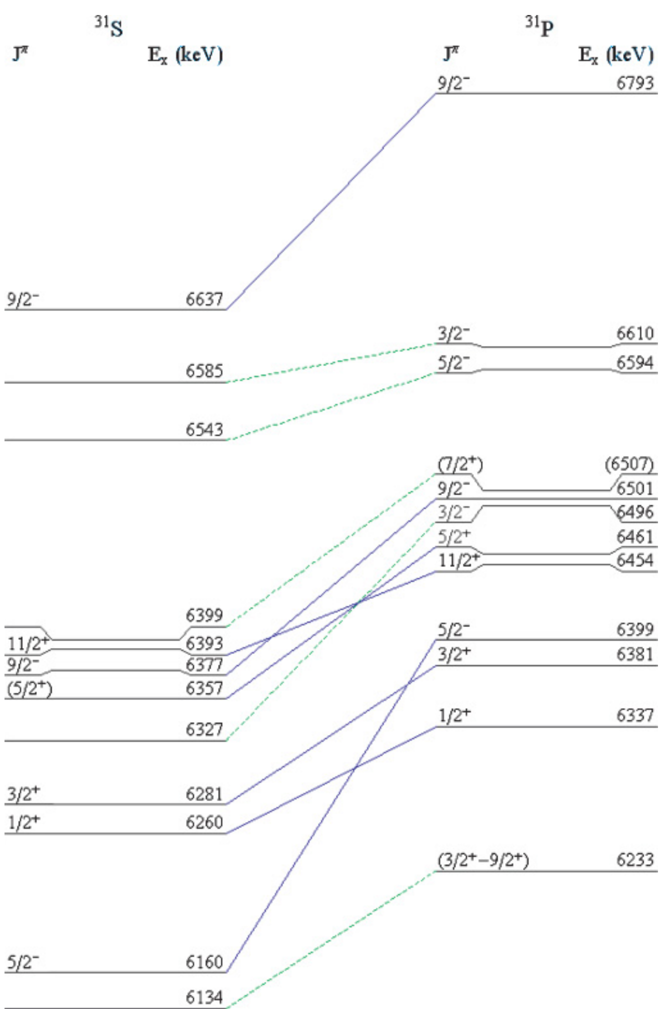

FIG. 2. (Color online) Level structure of ^{31}P and ^{31}S above the ^{30}P + p threshold at 6133 keV, including the present work. Solid (blue online) lines indicate mirror assignments from Refs. [14,21,22]. Dashed lines (green online) indicate additional mirror assignments used to derive ^{31}S J^π values for the rate calculation in the present work.

$0.12 < T < 0.18$ GK. The previously unidentified resonances at $E_r = 194.0(25)$ and 266.4(27) keV dominate the rate for $0.08 < T < 0.25$ GK under the present assumptions, spanning over half the range [1] of temperatures ($0.10 \leqslant T \leqslant 0.35$ GK) relevant to ONe novae. The $\ell = 0$ resonance at 126.9(23) keV

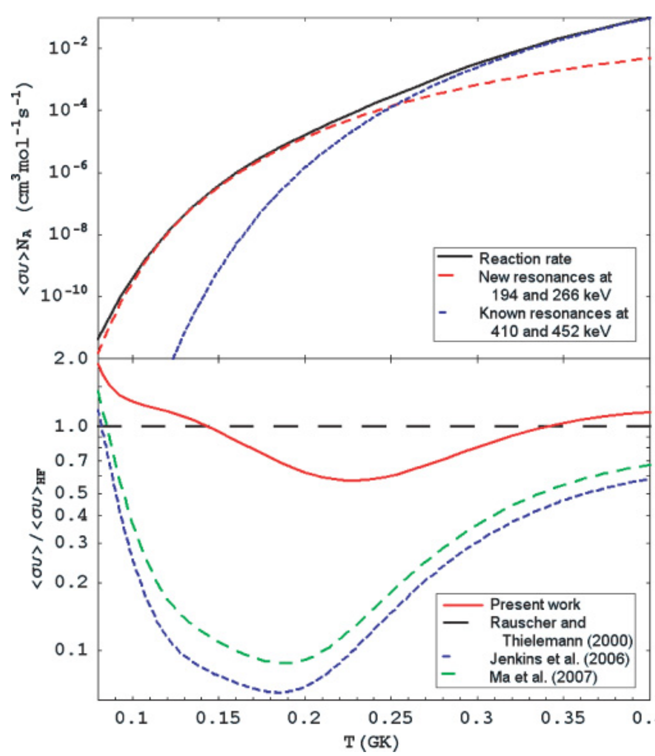

FIG. 3. (Color online) (Top) The astrophysical ^{30}P$(p,\gamma)^{31}$S reaction rate, showing the dominant contribution of the new resonances from the present work for $T < 0.25$ GK. (Bottom) The ratio of the experimental rates derived from the present work, Jenkins *et al*. [14], and Ma *et al*. [15] to the Hauser-Feshbach calculations of Rauscher and Thielemann [12]. Note that Fig. 3 in Ref. [14] is misplotted.

remains dominant for $0.02 < T < 0.08$ GK and the 410.1(25) and 452.1(25) keV resonances still dominate for $0.25 < T < 0.4$ GK. The 223.8(25) keV ($\ell = 2$) resonance now makes only a minor 2–11% contribution to the rate for $0.10 < T < 0.30$ GK.

Proton capture to the $T = 3/2, \ell = 0$, 148.2(21) keV resonance is isospin forbidden. It was included by suppressing the assumed C^2S value of 0.10 by a factor of 2.5×10^{-3} [14] and found to contribute <12% to the reaction rate. If isospin suppression is not so strong as assumed, this resonance might contribute significantly for $0.05 < T < 0.13$ GK.

The ^{30}P$(p,\gamma)^{31}$S rate from the present work is in accord with the rate derived from HF models [11,12] within a factor of 2 for $T > 0.08$ GK. This result is independent of the mirror partners chosen. Therefore any general conclusions drawn using these HF rates in hydrodynamic ONe nova models [7] are supported. In particular, despite the increase in the experimentally determined rate there remains a discrepancy between the ^{30}Si/^{28}Si ratios measured in presolar grains and those predicted for the ejecta of hydrodynamic models. At present this problem seems to require mixing of the initial ejecta with solar composition material prior to grain condensation, but this picture could change if any resonances are stronger than assumed.

Although the reduction in resonance energy uncertainties in this work has exponentially reduced the related uncertainty in the reaction rate, the resonance strengths used were influenced by partial widths that were necessarily approximated, resulting in a large uncertainty in the reaction rate calculation that is still difficult to quantify. Challenging experiments that measure resonance strengths directly using radioactive ^{30}P beams will ultimately determine the astrophysical ^{30}P$(p,\gamma)^{31}$S reaction rate. Precise resonance energies from the present work and proton branching ratios from future work [20] will minimize the time spent searching for resonances in direct measurements. In the meantime, the complementarity of high-resolution γ-ray measurements and nonselective reactions in nuclear astrophysics has been demonstrated.

We gratefully acknowledge the contributions of A. E. Champagne, F. Della Vedova, D. A. Hutcheon, R. Lewis, C. Westerfeldt, J. F. Wilkerson, and the WNSL staff. This work was supported by the U.S. Department of Energy under grant DE-FG02-91ER-40609.

[1] J. José, A. Coc, and M. Hernanz, Astrophys. J. **560**, 897 (2001).
[2] C. Iliadis *et al.*, Astrophys. J. Suppl. Ser. **134**, 151 (2001).
[3] M. A. J. Snijders *et al.*, Mon. Not. R. Astron. Soc. **228**, 329 (1987).
[4] J. Andreä, H. Drechsel, and S. Starrfield, Astron. Astrophys. **291**, 869 (1994).
[5] C. Morisset and D. Péquignot, Astron. Astrophys. **312**, 135 (1996).
[6] S. Amari *et al.*, Astrophys. J. **551**, 1065 (2001).
[7] J. José *et al.*, Astrophys. J. **612**, 414 (2004).
[8] E. Zinner, Annu. Rev. Earth Planet Sci. **26**, 147 (1998).
[9] W. Hauser and H. Feshbach, Phys. Rev. **87**, 366 (1952).
[10] G. R. Caughlan and W. A. Fowler, At. Data Nucl. Data Tables **40**, 283 (1988).
[11] F.-K. Thielemann, M. Arnould, and J. W. Truran, in *Advances in Nuclear Astrophysics, Proceedings of the Second IAP Workshop, Paris, France, 1986*, edited by E. Vangioni-Flam *et al.* (Gif-sur-Yvette, Editions Frontières), p. 525.
[12] T. Rauscher and F.-K. Thielemann, At. Data Nucl. Data Tables **79**, 47 (2001).
[13] C. Iliadis, *Nuclear Physics of Stars* (Wiley-VCH, Weinheim, 2007).
[14] D. G. Jenkins *et al.*, Phys. Rev. C **72**, 031303(R) (2005); **73**, 065802 (2006); (private communication).
[15] Z. Ma *et al.*, Phys. Rev. C **76**, 015803 (2007).
[16] G. Audi, A. H. Wapstra, and C. Thibault, Nucl. Phys. **A729**, 337 (2003).
[17] H.-S. Tzeng *et al.*, Nucl. Instrum. Methods **150**, 143 (1978).
[18] J. F. Wilkerson, Ph.D. thesis, University of North Carolina, 1982.
[19] A. Parikh, Ph.D. thesis, Yale University, 2006.
[20] C. Wrede *et al.* (to be submitted).
[21] P. M. Endt, Nucl. Phys. **A521**, 1 (1990); **A633**, 1 (1998).
[22] J. Vernotte *et al.*, Nucl. Phys. **A655**, 415 (1999).
[23] A. Kankainen *et al.*, Eur. Phys. J. A **27**, 67 (2006).
[24] F. Della Vedova *et al.*, Phys. Rev. C **75**, 034317 (2007); (private communication).
[25] C. E. Moss, Nucl. Phys. **A145**, 423 (1970).
[26] T. S. Bhatia, W. W. Daehnick, and G. J. Wagner, Phys. Rev. C **5**, 111 (1972).
[27] C. H. Bornman *et al.*, Nucl. Phys. **A112**, 231 (1968).
[28] P. M. Endt and C. van der Leun, Nucl. Phys. **A214**, 1 (1973).
[29] E. O. de Neijs *et al.*, Nucl. Phys. **A254**, 45 (1975).
[30] A. R. Barnett, Comput. Phys. Commun. **27**, 147 (1982).
[31] C. Iliadis, Nucl. Phys. **A618**, 166 (1997).